


Differences in Neural Crest Sensitivity to Ethanol Account for the Infrequency of Anterior Segment Defects in the Eye Compared with Craniofacial Anomalies in a Zebrafish Model of Fetal Alcohol Syndrome

Jessica Eason, Antionette L. Williams, Bahaar Chawla, Christian Apsey, and Brenda L. Bohnsack *

Background: Ethanol (ETOH) exposure during pregnancy is associated with craniofacial and neurologic abnormalities, but infrequently disrupts the anterior segment of the eye. In these studies, we used zebrafish to investigate differences in the teratogenic effect of ETOH on craniofacial, periocular, and ocular neural crest. **Methods:** Zebrafish eye and neural crest development was analyzed by means of live imaging, TUNEL (terminal deoxynucleotidyl transferase dUTP nick end labeling) assay, immunostaining, detection of reactive oxygen species, and in situ hybridization. **Results:** Our studies demonstrated that *foxd3*-positive neural crest cells in the periocular mesenchyme and developing eye were less sensitive to ETOH than *sox10*-positive craniofacial neural crest cells that form the pharyngeal arches and jaw. ETOH increased apoptosis in the retina, but did not affect survival of periocular and ocular neural crest cells. ETOH also did not increase reactive oxygen species within the eye. In contrast, ETOH increased ventral neural crest apoptosis and reactive oxygen species production in the facial mesenchyme. In the eye and craniofacial region, *sod2* showed high levels of

expression in the anterior segment and in the setting of *Sod2* knockdown, low levels of ETOH decreased migration of *foxd3*-positive neural crest cells into the developing eye. However, ETOH had minimal effect on the periocular and ocular expression of transcription factors (*pitx2* and *foxc1*) that regulate anterior segment development. **Conclusion:** Neural crest cells contributing to the anterior segment of the eye exhibit increased ability to withstand ETOH-induced oxidative stress and apoptosis. These studies explain the rarity of anterior segment dysgenesis despite the frequent craniofacial abnormalities in fetal alcohol syndrome.

Birth Defects Research 109:1212–1227, 2017.

© 2017 Wiley Periodicals, Inc.

Key words: neural crest; fetal alcohol syndrome; eye development; anterior segment; superoxide dismutase; ethanol; congenital eye disease

Introduction

Fetal alcohol spectrum disorders refer to the range of multi-systemic anomalies resulting from maternal alcohol consumption during pregnancy (Jones et al., 1973; Lemoine et al., 2003; Sokol, 2003; Hoyme et al., 2005; Riley et al., 2011). The most severe manifestation in this spectrum is referred to as fetal alcohol syndrome (FAS) and includes a combination of growth retardation, neurological deficits, and craniofacial malformations. The neuroepithelium, which forms the central nervous system, and the cranial neural crest, which gives rise to the bone and connective tissue of the craniofacial region, are tissues

that are highly sensitive to the effects of ethanol (ETOH) (Clarren et al., 1978; Mattson and Riley, 1996; Sampson et al., 1997; Kiecker, 2016; Lovely et al., 2016). In humans and animals, the effects of ETOH on brain and cranial neural crest development are closely related to the duration and concentration of exposure (Sulik et al., 1981; Riley et al., 2011; Joya et al., 2014; Zhang et al., 2014; Kiecker, 2016).

Numerous studies have demonstrated that ETOH alters the patterning of the neuroepithelium resulting in the inhibition of neuronal induction, proliferation, and survival (Sulik et al., 1984; Maier et al., 1997, 1999; Dunty et al., 2002; Parnell et al., 2009; Zhang et al., 2016). These alterations commonly disrupt neurological function and behavior, and in severe cases, lead to structural abnormalities, such as agenesis of the corpus callosum and cerebellar hypoplasia (Mattson and Riley, 1996; Lemoine et al., 2003; Sokol, 2003; Hoyme et al., 2005; Riley et al., 2011). In the adjacent neural crest, early exposure to ETOH decreases delamination, inhibits proliferation, decreases survival, and alters migration (Garic-Stankovic et al., 2005; Flentke et al., 2011; Garic et al., 2011; Smith et al., 2014; Tolosa et al., 2016), resulting in the classic craniofacial anomalies associated with FAS (e.g., thin vermilion, shortened palpebral fissures, and smooth philtrum), and also causing cleft

Additional Supporting information may be found in the online version of this article.

Supported by the National Eye Institute of the National Institutes of Health; KO8EY022912-01.

Vision Research Core; P30 EY007003.

Department of Ophthalmology and Visual Sciences, Kellogg Eye Center, University of Michigan, Ann Arbor, Michigan

*Correspondence to: Brenda L. Bohnsack, Department of Ophthalmology and Visual Sciences, Kellogg Eye Center, University of Michigan, 1000 Wall Street, Ann Arbor, MI 48105. E-mail: brenbado@med.umich.edu

Published online 6 July 2017 in Wiley Online Library (wileyonlinelibrary.com).
Doi: 10.1002/bdr2.1069

lip and cleft palate in severe cases (Hoyme et al., 2005; Klingenberg et al., 2010; Riley et al., 2011; Foroud et al., 2012).

The cranial neural crest, which arises from the prosencephalon, mesencephalon, and rhombencephalon, follows specific migratory pathways into the craniofacial region (Trainor and Tam, 1995; Trainor, 2005; Bohnsack and Kahana, 2013; Chawla et al., 2016). At the same time that the jaw and pharyngeal arches are forming, a subgroup of neural crest cells, which initially populates the periocular mesenchyme, enters the eye (Johnston, 1966; Johnston et al., 1979; Creuzet et al., 2005). In other congenital disorders (e.g., Axenfeld-Rieger syndrome and Peters Plus syndrome), craniofacial anomalies are associated with malformations of the anterior segment of the eye (Ozeki et al., 1999; Lesnik Oberstein et al., 2006; Strungaru et al., 2007; Tumer and Bach-Holm, 2009; Aliferis et al., 2010; Dressler et al., 2010; Schoner et al., 2013). Of interest, corneal, iris, and angle abnormalities are a rare manifestation of FAS (Miller et al., 1984; Stromland, 1987; Chan et al., 1991; Edward et al., 1993; Brennan and Giles, 2014). The molecular differences between neural crest cells that give rise to craniofacial structures versus neural crest cells that form the anterior segment are not well defined. Differences in sensitivity to ETOH suggest that the periocular and ocular neural crest are molecularly distinct from the craniofacial neural crest. Although numerous studies have investigated the effect of ETOH on the cranial neural crest in facial development, few studies have focused on the periocular and ocular populations.

In the present study, we used a zebrafish model of FAS to investigate the effects of ETOH exposure on the periocular and ocular neural crest. The neural crest cells that enter the eye have been difficult to study, reflecting their transient nature and the lack of adequate markers to track this migrating population. We identified *foxd3* as a marker for these cells within zebrafish embryos and larvae in contrast to *sox10*, which was predominantly detected in craniofacial neural crest cells. Using these two markers, we investigated differences in cell survival, reactive oxygen species (ROS) production, and gene expression in response to ETOH exposure in these neural crest cell populations.

Materials and Methods

ANIMAL CARE/ANIMAL STRAINS

Zebrafish (*Danio rerio*) were raised in a breeding colony under a 14-hr light/10-hr dark cycle as previously described (Bohnsack et al., 2011a, 2011b, 2012; Bohnsack and Kahana, 2013; Chawla et al., 2016). Embryos were maintained at 28.5 degrees Celsius and staged as previously described (Kimmel et al., 1995). The transgenic strains Tg(*sox10:EGFP*), Tg(*sox10:mRFP*), and Tg(*foxd3:GFP*) were gifts from Thomas Schilling, Cunming Duan, and

Mary Halloran, respectively, and the strains were crossed into the *Roy* (*roy* $-/-$) or *Casper* (*roy* $-/-$, *nacre* $-/-$) background to decrease auto-fluorescence and interference resulting from pigmentation (Dutton et al., 2001a, 2001b; Kucenas et al., 2008; Curran et al., 2009). Animal protocols were performed in accordance with the guidelines for the humane treatment of laboratory animals established by the University of Michigan Committee on the Use and Care of Animals (IACUC, protocol #10205) and the ARVO (Association for Research in Vision and Ophthalmology) Statement for the Use of Animals in Ophthalmic and Vision Research.

IMAGING

Whole embryos were analyzed using a M205FA combi-scope (Leica Microsystems CMS GmbH, Germany, Wetzlar, Germany). Images were obtained using brightfield DFC290 (Leica) and fluorescent ORCA-ER (Hamamatsu, Hamamatsu City, Japan) cameras. The sections were imaged using a DM6000B upright microscope (Leica) equipped with a DFC500 camera (Leica). The images were processed and analyzed using Adobe Photoshop (San Jose, CA), LAS X (Leica), and/or LAS AF6000 software (Leica). The images shown are representative of all experiments. For quantifying the number of *foxd3*-positive periocular mesenchymal and ocular neural crest cells, z-stacks that ranged from the lateral edge of the cornea to 100 μ m medial to the medial edge of the eye were obtained. The z-stacks were deconvolved and maximally projected to obtain a single image. The number of *foxd3*-positive cells was manually counted. Eye size was measured from the dorsal to ventral border in a lateral view and from the anterior to posterior border in a ventral view. Measurements were obtained from bilateral eyes of four to six embryos at each time point for each group. The data were statistically analyzed using ANOVA with Tukey's posthoc analysis, and $p < 0.05$ was considered statistically significant.

PHARMACOLOGICAL TREATMENTS

Absolute ethanol (ETOH, Sigma-Aldrich, St. Louis, MO) was administered in the embryo media at 0.5 to 3%. The embryos were dechorionated, and the treatments were administered from 24 to 48 hr postfertilization (hpf). Following treatment, the embryos were washed multiple times with embryo media and subsequently placed in fresh embryo media for the remainder of the time course as indicated. Experiments used 50 to 100 embryos per treatment group and were replicated 4 to 6 times. Phenotypes were assessed at 36, 48, 60, and 72 hpf. Data were statistically analyzed using ANOVA with Tukey's post hoc analysis. A p value of <0.5 was considered statistically significant.

MORPHOLINO OLIGONUCLEOTIDE INJECTIONS

Translation blocking (GAACATATCCGACTCTGCACAGCAT) and five-basepair mismatch control (GAAGAAATCGGACTCT

CCACACCAT) antisense morpholino oligonucleotides (MO; Gene Tools, LLC Corvallis, OR) directed against zebrafish *Sod2* were reconstituted in de-ionized water. The sequences for the MO were previously published (Peterman et al., 2015). Concentrations yielding consistent and reproducible phenotypes were determined for each MO. One-cell stage embryos were injected with 1 to 2 nl of MO at a concentration of 0.25 mM (2.1 ng/nl). Embryos were imaged at 24, 36, 48, and 60 hpf as described above.

METHYLACRYLATE SECTIONS

Zebrafish embryos at 96 hpf were fixed in 2% paraformaldehyde/1.5% glutaraldehyde overnight at 4°C, followed by embedding in methylacrylate. The blocks were sectioned at 5 μ m. The sections were stained with Lee's stain and imaged as described above.

IMMUNOSTAINING AND TUNEL ASSAY

The staged zebrafish embryos were fixed in 4% paraformaldehyde overnight at 4°C. Whole-mount immunostaining for green fluorescent protein (GFP) and terminal deoxynucleotidyl transferase dUTP nick end labeling (TUNEL) assays were performed as previously described using standard protocols (Bohnsack and Kahana, 2013). Briefly, apoptotic cells were detected through the TdT-mediated incorporation of digoxigenin-labeled deoxyuridine triphosphate. Sheep anti-digoxigenin conjugated to rhodamine was used to detect the TUNEL signal. The embryos were subsequently incubated with mouse anti-GFP directly conjugated to FITC (1:200, Millipore, Billerica, MA). The embryos were cryoprotected in successive sucrose solutions, embedded in Optimal Cutting Temperature (O.C.T) compound, and subsequently sectioned at 10 μ m. The sections were co-stained with DAPI (4',6-diamidino-2-phenylidole-dihydrochloride) and imaged as described above.

For quantification of the percentage of cells undergoing apoptosis in the eye at 48 hpf, 3 consecutive sections through the equator of the lenses of at least 4 embryos per group were included. The number of cell nuclei as marked by DAPI staining and the number of TUNEL-positive cells in the eyes were manually counted. The data were statistically analyzed using ANOVA with Tukey's post-hoc analysis, and $p < 0.05$ was considered statistically significant.

For *Sod2* immunostaining, embryos were harvested at 48 hpf, fixed in 4% paraformaldehyde, and cryoprotected in successive sucrose solutions. Embryos were embedded in O.C.T. compound and sectioned at 10 μ m. The sections were washed in phosphate buffered saline (PBS), dehydrated in acetone, and blocked in 10% normal goat serum in PBS with 0.1% Triton. Sections were incubated with anti-*Sod2* (1:100, Genetex, Irvine, CA) overnight at 4°C. The sections were washed in PBS and then incubated with goat anti-rabbit secondary antibody conjugated to Cy3

(1:1000, Abcam, Cambridge, MA) for 2 hr at room temperature. The sections were washed, costained with DAPI, and imaged as described above.

DETECTION OF ROS

Tg(*sox10:mRFP*) embryos were incubated with CellROX Green Reagent (Molecular Probes, Life Technologies, Carlsbad, CA) at a final concentration of 5 μ M in embryo media for 30 min in the dark before harvesting in 4% paraformaldehyde at 26 hpf (Mugoni et al., 2014). The embryos were cryoprotected in successive sucrose solutions, embedded in O.C.T., and sectioned at 10 μ m. The sections were immediately co-stained with DAPI and imaged as described above.

RT-PCR

Total mRNA from 48 hpf embryos was isolated using the ReliaPrep RNA Tissue Miniprep System (Promega, Madison, WI) and quantified using Nanodrop 2000 (Thermo Scientific, Willmington, DE) spectrophotometry. One microgram of RNA was reverse transcribed using Superscript IV Reverse Transcriptase (ThermoFisher Scientific, Waltham, MA). The primer sequences for *sod1*, *sod2*, *sod3*, *pitx2a*, *foxc1a*, *foxc1b*, and β -*actin* are listed in Supplementary Table 1, which is available online. For semi-quantitative RT-PCR, cycle optimization was performed to determine the linear range of each primer set (Supplementary Table 1). PCR was performed using Platinum Taq (ThermoFisher), and the products were detected on 2% agarose gels. Each experiment was repeated four times, and the images shown are representative of all experiments.

IN SITU HYBRIDIZATION

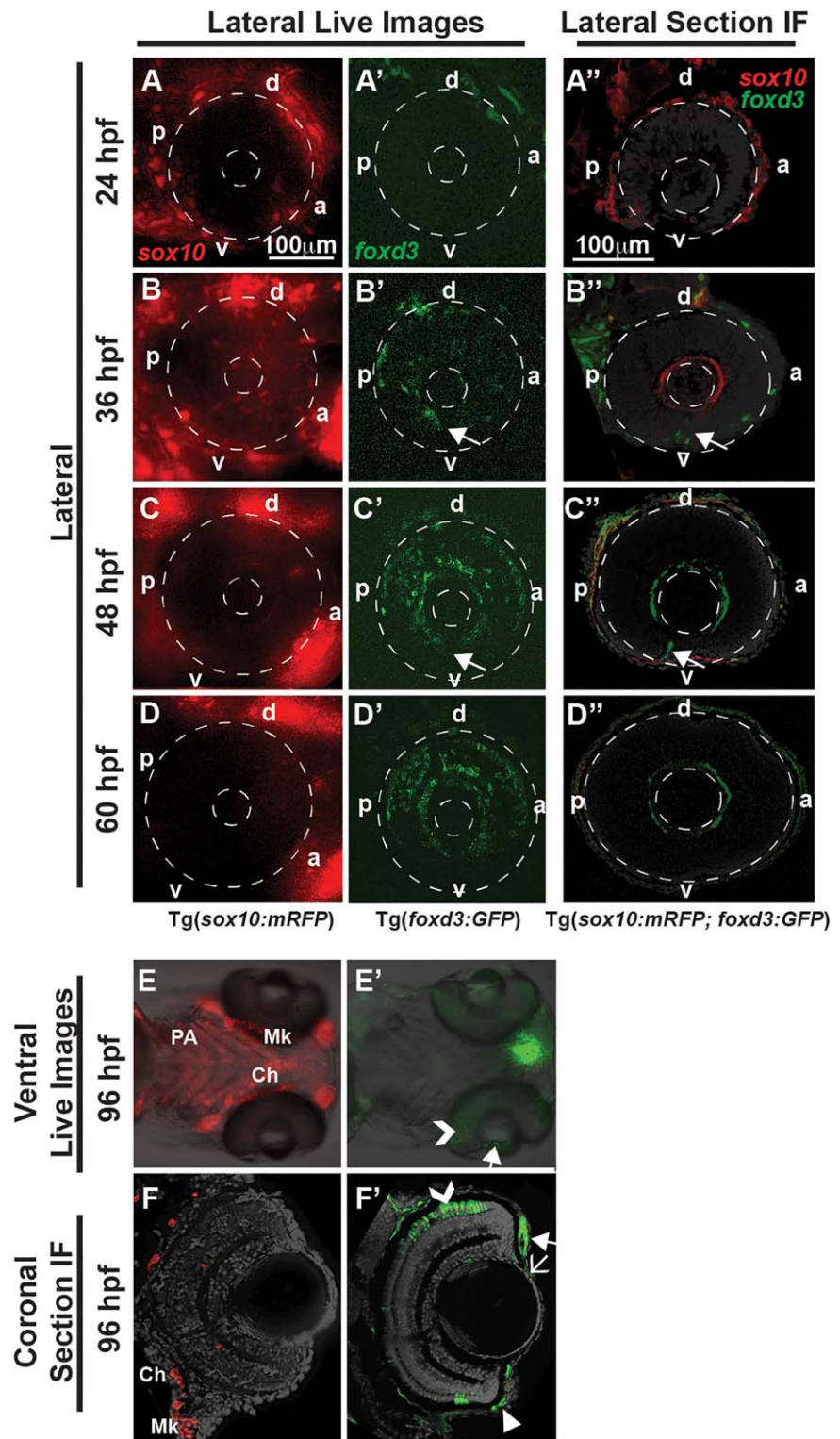
In situ hybridization was performed through standard protocols using digoxigenin-labeled RNA antisense probes (Barthel and Raymond, 2000; Bohnsack et al., 2011b). For colorimetric reactions, the embryos were developed for equal amounts of time. Sense controls were also developed in parallel to ensure specific staining.

Results

MIGRATION OF CRANIOFACIAL AND PERIOcular NEURAL CREST SHOWED DIFFERENT SENSITIVITIES TO ETOH

Traceable differences between the cranial neural crest cells that give rise to the craniofacial structures versus those that contribute to the anterior segment of the eye were determined using the Tg(*sox10:mRFP*), Tg(*foxd3:GFP*), and Tg(*sox10:mRFP; foxd3:GFP*) transgenic lines. The transcription factors *sox10* and *foxd3* have been shown in numerous animal models to regulate early neural crest differentiation and are markers for neural crest cells (Dutton et al., 2001b; Honoré et al., 2003; Montero-Balaguer et al., 2006; Stewart et al., 2006; Kwak et al., 2013). In the present study, we observed that *sox10* and *foxd3*

FIGURE 1. *Sox10* and *foxd3* demarcated temporally and spatially distinct neural crest cells. Live imaging and lateral section immunofluorescence (IF) of 24 to 60 hpf *Tg(sox10:mRFP)*, *Tg(foxd3:GFP)*, and *Tg(sox10:mRFP; foxd3:GFP)* embryos showed the expression and migration patterns of *sox10* and *foxd3*-positive cells in the periocular mesenchyme and developing anterior segment. *Sox10* was highly expressed in the periocular mesenchyme at 24 hpf (A,A''), but showed decreased expression by 60 hpf (B–D,B'–D'). A small proportion of *sox10*-positive cells migrated into the eye between the surface ectoderm and optic cup from 24 to 48 hpf (A–C,A'–C''). Few *sox10*-positive cells were observed in the anterior segment at 60 hpf (D). Ventral live imaging (E) and coronal IF sections (F) showed *sox10*-positive cells in the craniofacial structures (pharyngeal arches [PA], ceratohyal cartilage [Ch], and Meckel's cartilage [Mk]), but not in the developing anterior segment, at 96 hpf. *Foxd3*-positive cells predominantly migrated into the anterior segment in the dorsal (d)-posterior (p) quadrant between the surface ectoderm and optic cup from 30 to 60 hpf (A'–D'). In addition, *foxd3*-positive cells migrated through the ocular fissure between 30 and 48 hpf (arrows, B',B'',C',C''). At 96 hpf, *foxd3* expression (E',F') was localized to the iris stroma (closed arrows, E',F'), cornea (open arrow, F'), and aqueous outflow tracts (closed arrowhead, F'), but was not expressed in the pharyngeal arches, Meckel's cartilage, or ceratohyal cartilage. *Foxd3* was expressed in retinal photoreceptors (open arrowhead, E',F') at 96 hpf, but this expression was not related to neural crest cells. Section analysis showed little overlap in expression of *sox10* and *foxd3* in neural crest cells entering the anterior segment (A'–D'). a, anterior; d, dorsal; p, posterior; v, ventral.



predominantly demarcated separate neural crest cell populations in the periocular mesenchyme and within the eye (Fig. 1A''–D'').

Only a small proportion of neural crest cells entering the eye were *sox10*-positive (Fig. 1A–D). These *sox10*-positive cells migrated between the optic cup and surface

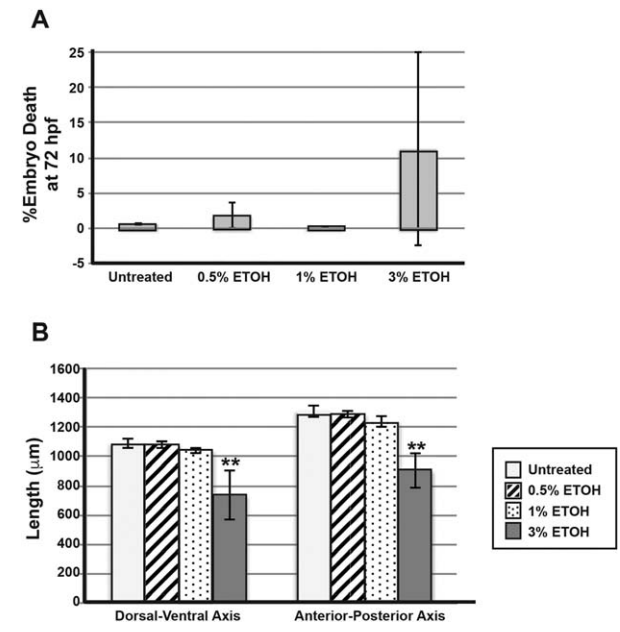


FIGURE 2. ETOH treatment from 24 to 48 hpf did not significantly affect embryonic survival, but did inhibit eye size. Treatment with 0.5%, 1%, or 3% ETOH from 24 to 48 hpf did not significantly increase the percentage of embryo death assessed at 72 hpf (**A**). Treatment with 0.5% or 1% ETOH did not significantly affect the length (in μm) of the eye in either the dorsal-ventral or anterior-posterior axis (**B**). However, treatment with 3% ETOH significantly decreased the eye size in both the dorsal-ventral and anterior-posterior axes compared with untreated embryos (**B**). * $p < 0.05$.

ectoderm, peaking at approximately 36 hpf. *Sox10* was no longer detected in the anterior segment after 60 hpf (Fig. 1D, D', and F), but maintained expression in the jaw and pharyngeal arches at 96 hpf (Fig. 1E and F). As previously demonstrated, *foxd3* marked a higher proportion of neural crest cells that entered the eye (Fig. 1A'-D') (Williams et al., 2017). *Foxd3*-positive cells migrated between the optic cup and surface ectoderm (arrows, Fig. 1B', C', B'', and C'') and through the ocular fissure (arrow). *Foxd3*-positive cells coalesced around the lens and contributed to the iris stroma (closed arrows, Fig. 1E' and F'), corneal stroma (Fig. 1F', open arrow), and aqueous outflow channels (Fig. 1F', closed arrowhead) at 96 hpf. *Foxd3* was not expressed in the jaw or pharyngeal arches at 96 hpf (Fig. 1E'). *Foxd3* was also detected in differentiated photoreceptors (Fig. 1E' and F', open arrowheads), but this expression was not related to neural crest cells. Thus, *sox10* and *foxd3* demarcated different neural crest cell populations that give rise to the jaw/pharyngeal arches and anterior segment structures, respectively.

To determine the effect of ETOH on anterior segment formation, Tg(*foxd3:GFP*) embryos were treated with increasing concentrations of ETOH (0.5%, 1%, and 3%) between 24 and 48 hpf and subsequently live imaged.

This time frame occurs after early neural crest migration into the craniofacial region and optic cup formation and during neural crest migration into the anterior segment of the eye. Treatment with 0.5% or 1% ETOH between 24 and 48 hpf did not decrease embryo survival at 72 hpf compared with untreated embryos (Fig. 2A) or significantly affect eye size (Fig. 2B; Supplementary Table 2) as measured along the dorsal-ventral and anterior-posterior axes. In the eye, 0.5% (data not shown) or 1% ETOH (Fig. 3B'-E') did not decrease *foxd3*-positive cells in the periocular mesenchyme (arrowheads) or alter ocular neural crest migration (closed arrows) between 24 and 72 hpf compared with untreated controls (Fig. 3A-E). Furthermore, 1% ETOH did not affect photoreceptor expression of *foxd3* at 72 hpf (open arrows, Fig. 1E'). At 96 hpf, methacrylate sections showed that 1% ETOH did not affect iris stroma formation (arrowheads, Fig. 3F') compared with untreated embryos (Fig. 3F). In contrast, treatment of Tg(*sox10:EGFP*) embryos with 1% ETOH from 24 to 48 hpf (Fig. 3G') showed delayed development of the pharyngeal arches (PA), ceratohyal (CH) cartilage, and Meckel's (Mk) cartilage at 96 hpf compared with untreated controls (Fig. 3G).

Treatment with 3% ETOH from 24 to 48 hpf significantly decreased eye size in both the dorsal-ventral and anterior-posterior axes (Fig. 2B; Supplementary Table 2). However, 3% ETOH from 24 to 48 hpf did not significantly decrease embryo survival at 72 hpf ($p = 0.81$). In Tg(*foxd3:GFP*) embryos this higher concentration of ETOH significantly decreased the number of *foxd3*-positive neural crest cells in the periocular mesenchyme (arrowheads, Fig. 3B''-D'') and in the developing eye (arrows, Fig. 3B''-E'') at 48 hpf compared with untreated and 1% ETOH treated embryos (Supplementary Table 3; Fig. 3B''-E'', H). However, there were *foxd3*-positive cells that migrated into the anterior segment (thin arrow, Fig. 3E'') between 36 and 72 hpf. Although the eyes were smaller with misshapen lenses, the neural crest cells formed iris stroma (arrowheads, Fig. 3F'') and corneal stroma (arrow, Fig. 3F'') at 96 hpf. Treatment of Tg(*sox10:EGFP*) embryos with 3% ETOH resulted in severe malformation of pharyngeal arch, ceratohyal, and Meckel's cartilage at 96 hpf (Fig. 3G''). Thus, periocular and ocular neural crest cells are less sensitive to ETOH compared with the neural crest cell population that gives rise to the craniofacial cartilages.

ETHANOL INDUCED APOPTOSIS IN THE RETINA, LENS, AND FACIAL MESENCHYME

Previous studies have shown that ETOH increases craniofacial neural crest apoptosis, but the effects of ETOH on the survival of the neural crest inside and around the eye have not been determined (Garic-Stankovic et al., 2005; Smith et al., 2014). TUNEL assay in Tg(*sox10:EGFP*) and Tg(*foxd3:GFP*) embryos demonstrated that 1% ETOH starting at 24 hpf significantly increased the percentage of

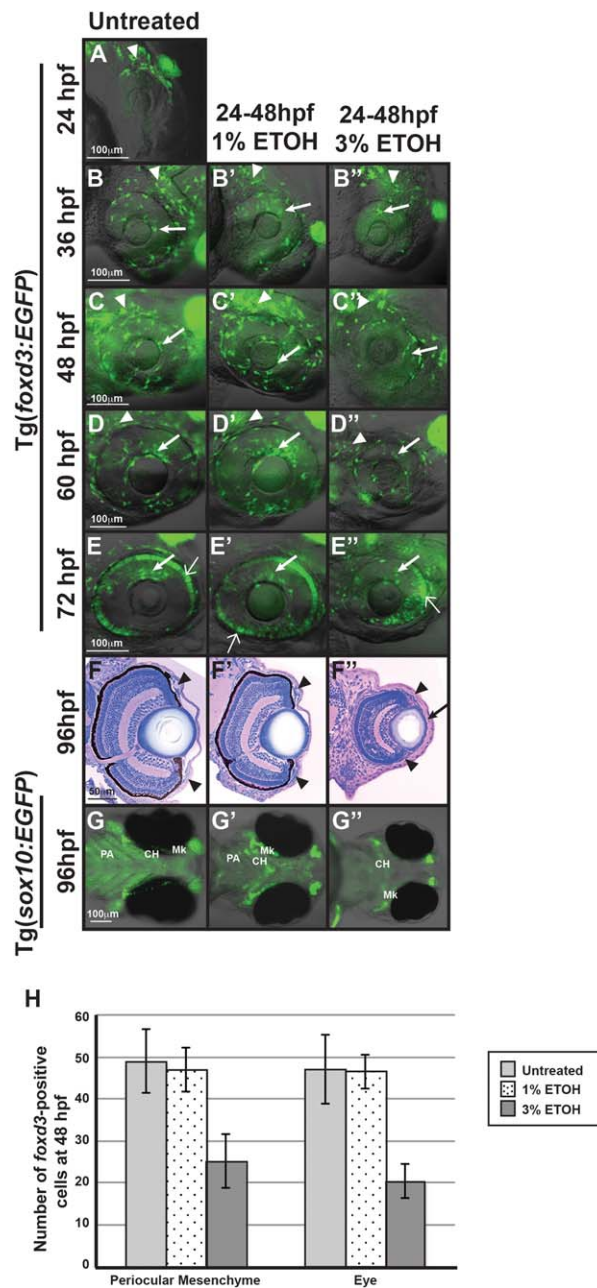


FIGURE 3. Craniofacial neural crest cells were more sensitive to ETOH than periocular and ocular neural crest cells. Live imaging of *Tg(foxd3:GFP)* embryos from 24 (A) to 72 hpf demonstrated that treatment with 1% ETOH from 24 to 48 hpf (B'–E') did not alter the migration of *foxd3*-positive cells between the surface ectoderm and optic cup (closed arrows) or through the ocular fissure compared with untreated controls (B–E). In addition, 1% ETOH did not affect the number of *foxd3*-positive cells in the periocular mesenchyme (arrowheads, B'–D';H) and did not affect photoreceptor expression of *foxd3* (open arrows, E'). Methylacrylate sections of 96 hpf embryos showed that 1% ETOH treatment from 24 to 48 hpf did not affect iris stroma cellularity (arrowheads, F') compared with untreated embryos (F). In contrast, live imaging of *Tg(sox10:EGFP)* embryos at 96 hpf showed that treatment with 1% ETOH from 24 to 48 hpf (G') delayed Meckel's (Mk) cartilage, ceratohyal (CH), and pharyngeal arch (PA) cartilage formation compared with untreated controls (G). Treatment with 3% ETOH from 24 to 48 hpf caused developmental delay by 36 hpf (B'') and at 48 hpf significantly decreased the number of *foxd3*-positive cells present in the periocular mesenchyme (arrowhead, C'';H). Furthermore, there were fewer *foxd3*-positive cells in the developing eye (closed arrows, B''–E'') of 36 to 72 hpf embryos treated with 3% ETOH. However, analysis of methylacrylate sections at 96 hpf (F'') showed that neural crest cells were present in the iris stroma (arrowheads) and corneal stroma (arrow), although the corneas were thickened and the lenses were misshapen. Treatment with 3% ETOH inhibited *sox10*-positive neural crest cell-derived pharyngeal arch formation and resulted in ceratohyal and Meckel's cartilage malformation (G'').

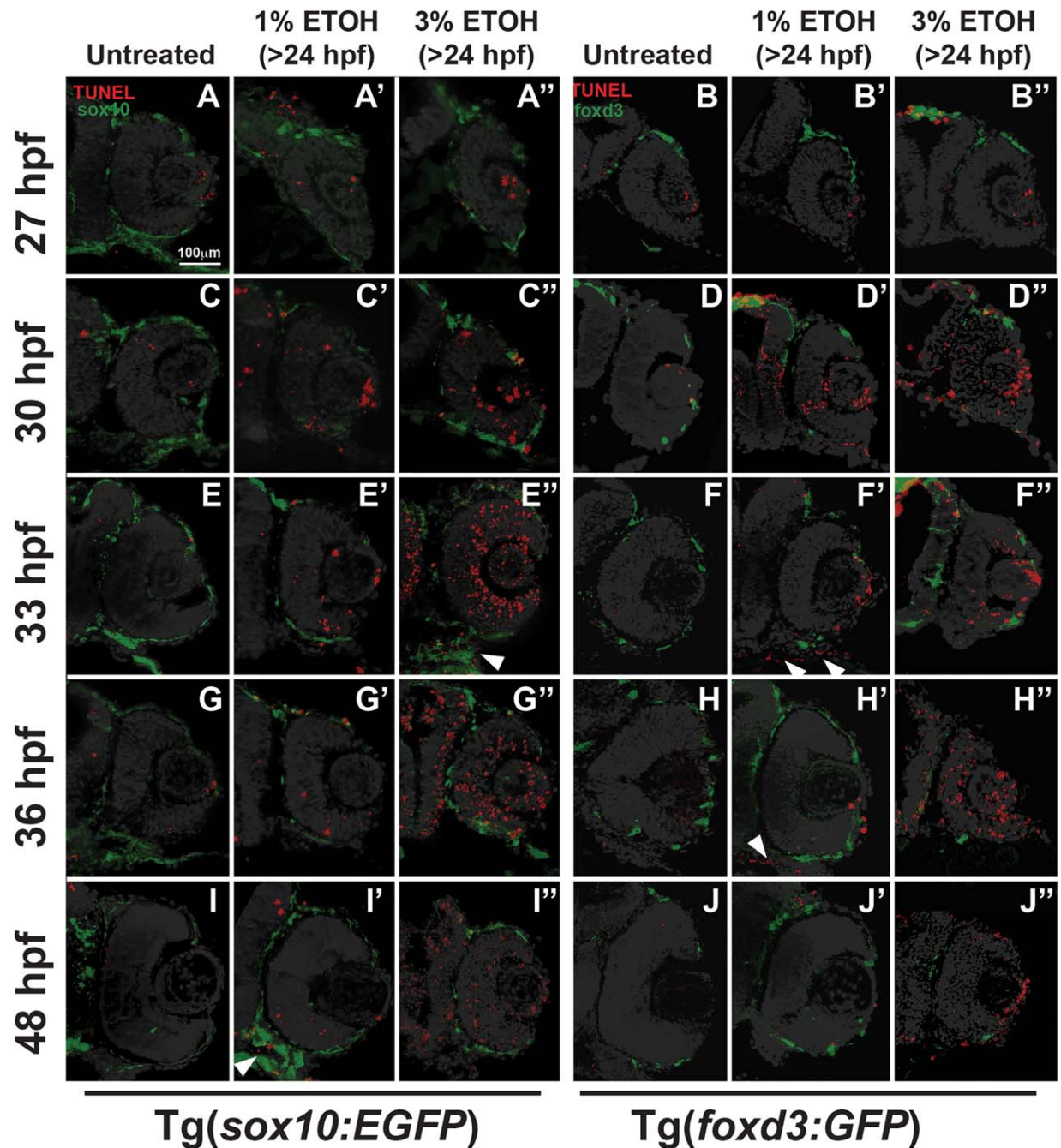


FIGURE 4. ETOH increased apoptosis in craniofacial neural crest cells but not ocular neural crest cells. TUNEL assay on sections from 27 to 48 hpf Tg(sox10:EGFP) or Tg(foxd3:GFP) embryos demonstrated that treatment with 1% ETOH starting at 24 hpf caused a transient increase in apoptosis within the eye at 30 (C',D') and 33 (E',F') hpf compared with untreated embryos (C-F). The apoptosis was not localized to either sox10-positive or foxd3-positive cells within the eye. In contrast, 1% ETOH did not affect cell survival in the developing eye at 27 (A,B'), 36 (G,H'), or 48 (I,J') hpf. Treatment with 3% ETOH starting at 24 hpf caused a significant decrease in cell survival within the eye (A''-J''), but this apoptosis was not specifically localized to sox10- or foxd3-positive cells in the ocular neural crest. In contrast, 1% or 3% ETOH increased apoptosis in sox10-positive cells (arrowheads, E'' I') in the facial mesenchyme (arrowheads, F' and H').

apoptotic cells in the developing eye at 30 (Fig. 4C' and D') and 33 (Fig. 4E' and F'; Fig. 5; Supplementary Table 4) hpf compared with untreated controls (Fig. 4C-F). The

apoptotic cells in the eyes were not specifically localized to sox10 or foxd3-positive neural crest cells in the periocular mesenchyme or the eye. Treatment with 1% ETOH did

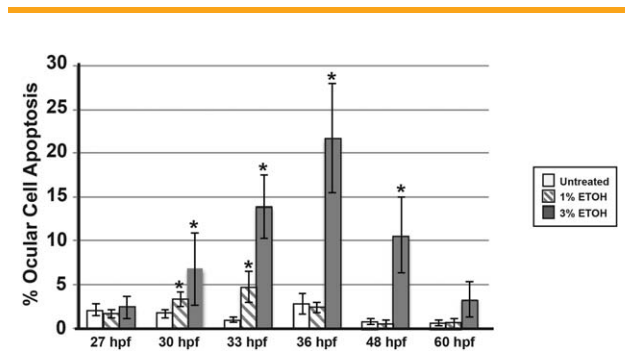


FIGURE 5. ETOH significantly increased apoptosis within the developing eye. Treatment with 1% ETOH from 24 to 48 hpf showed a transient increase in the percentage of apoptotic cells within the developing eye at 30 and 33 hpf. Treatment with 3% ETOH significantly increased the percentage of apoptotic cells in the eye after 6 hr, and this effect continued through 48 hpf.

not affect cell survival at 27 (Fig. 4A' and B'), 36 (Fig. 4G' and H'), and 48 (Fig. 4I' and J') hpf compared with untreated controls (Fig. 4E–J). Between 30 and 48 hpf, apoptotic cells were also observed in the jaw mesenchyme (arrowheads, Fig. 4F', H', and I'). Treatment with 3% ETOH starting at 24 hpf significantly increased the percentage of apoptotic cells in the developing eye from 30 to 48 hpf (Fig. 4C''–J''; Fig. 5; Supplementary Table 4). In 3% ETOH-treated embryos, the cells undergoing apoptosis were located throughout the eye, particularly in the retina and lens (Fig. 4C'' and D''). These findings show that ETOH induced apoptosis in the neural crest in the facial mesenchyme, but spared the neural crest in the anterior segment of the eye.

ETHANOL INCREASED OXIDATIVE STRESS IN THE FACIAL MESENCHYME, BUT NOT THE OCULAR NEURAL CREST

Ethanol-induced apoptosis in the cranial neural crest and neuroepithelium has previously been attributed in part to an increase in oxidative stress (Davis et al., 1990; Floyd and Carney, 1992; Henderson et al., 1995; Chen et al., 2000). Using Tg (*sox10:mRFP*) embryos, we investigated whether ETOH exposure increased ROS in and around the eye. Within 2 hours of ETOH exposure (1% or 3%), increased ROS was observed in the *sox10*-positive ventral neural crest cells, which forms the facial mesenchyme (arrows, Fig. 6B and C), compared with untreated controls (Fig. 6A). However, there was no increased ROS within the developing eye.

Superoxide dismutase enzymes, namely *sod1*, *sod2*, and *sod3*, are important antioxidant molecules that catalyze the conversion of ROS to less harmful byproducts (Koch et al., 1991, 1994, 2004; Kajimura et al., 2005). To investigate the resistance of periocular and ocular neural crest cells to oxidative stress-induced by ETOH, the expression of the *sod* genes in and around the developing eye was next determined. In situ hybridization at 36 hpf showed that all of the *sod* enzymes were expressed within the

hyaloid vasculature (arrowheads, Fig. 6D–F) and periocular mesenchyme. *Sod1* and *sod3* were also expressed within the retina and facial mesenchyme (open arrow, Fig. 6D), while *sod2* was the predominant enzyme in the anterior segment. *Sod2* was expressed in lens epithelial cells and the neural crest cells between the optic cup and surface ectoderm (arrow, Fig. 6E').

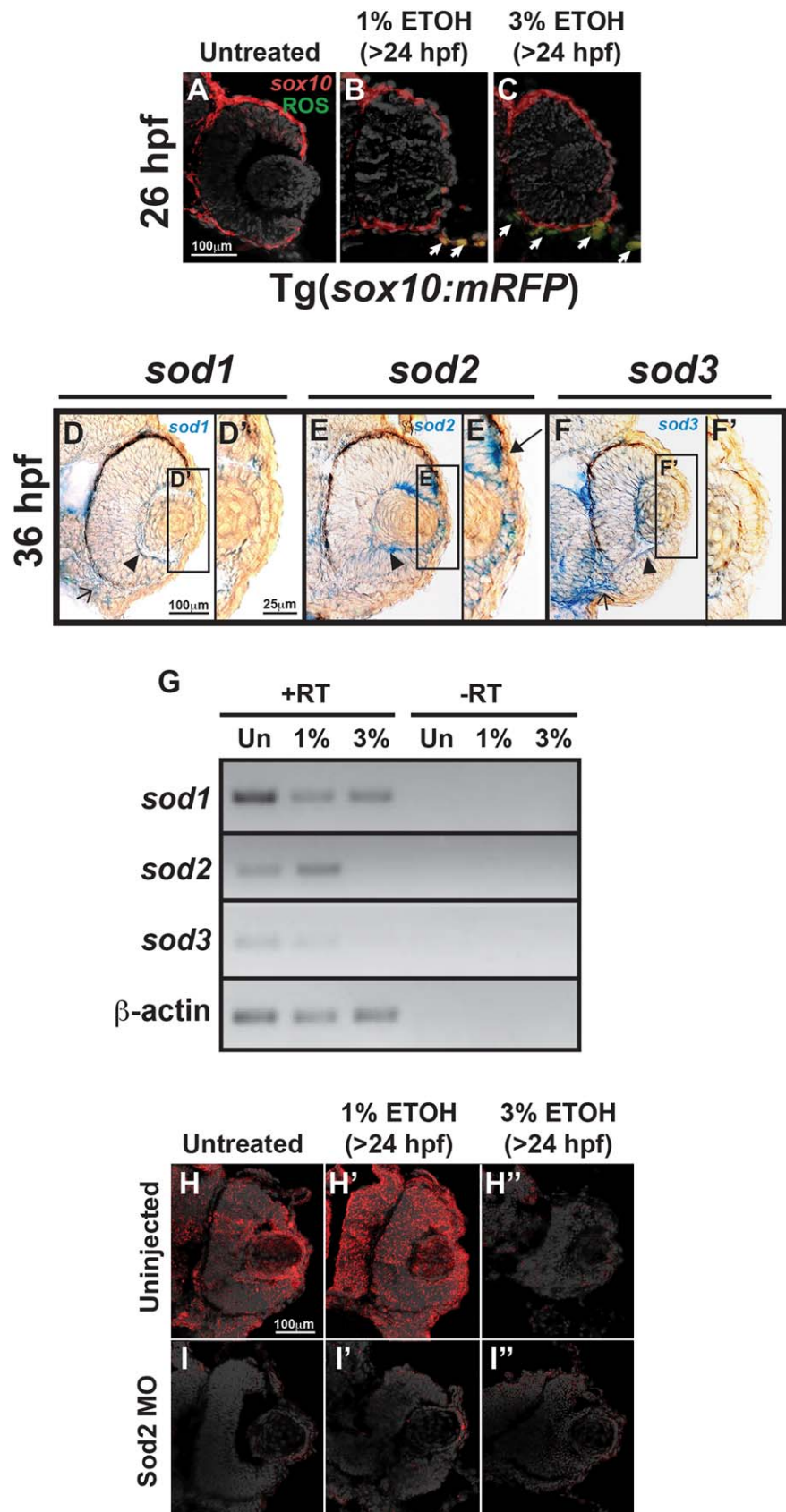
Semi-quantitative RT-PCR of RNA from whole 48 hpf embryos revealed that treatment with 1% or 3% ETOH starting at 24 hpf decreased the overall transcript expression of *sod1* and *sod3* compared with untreated controls (Fig. 6G). Notably, 1% ETOH increased *sod2* expression at 48 hpf, whereas treatment with 3% ETOH decreased *sod2* expression. Immunohistochemistry confirmed protein expression of Sod2 within the anterior segment (Fig. 6H) and further showed that protein levels were increased by 1% ETOH (Fig. 6H'), but decreased by 3% ETOH exposure (Fig. 6H''). Thus, the developing eye has regional expression of *sod* enzymes that are differentially regulated by ETOH exposure.

Because Sod2 was expressed in the anterior segment, the effect of this enzyme on the ocular neural crest was determined. Knockdown of Sod2 (using MO injected into 1-cell stage Tg[*foxd3:GFP*] embryos) did not affect *foxd3*-positive cell migration into the anterior segment between 36 and 72 hpf (closed arrows, Fig. 7E–H) compared with mismatch control-injected (Fig. 7A–D) and uninjected (Fig. 3B–E) embryos. Immunohistochemistry (Fig. 6I) confirmed that MO injection decreased Sod2 protein expression at 48 hpf in whole embryos and within the anterior segment. In the setting of Sod2 MO knockdown, treatment with 1% ETOH from 24 to 48 hpf decreased *foxd3*-positive neural crest cell migration into the anterior segment (closed arrows, Fig. 7E'–H'). However, there were still *foxd3*-positive cells in the periocular mesenchyme (arrowheads, Fig. 7E'–G'). This was in contrast to mismatch control-injected (Fig. 7A'–D') or uninjected (Fig. 3B'–E') embryos in which 1% ETOH did not affect *foxd3*-positive cell migration into the anterior segment. Treatment with 3% ETOH between 24 and 48 hpf decreased *foxd3*-positive cells in the periocular mesenchyme (arrowheads) and in the developing eye in Sod2 knockdown (Fig. 7E''–H''), mismatch control-injected (Fig. 7A''–D''), and uninjected (Fig. 3B''–E'') embryos. These results show that Sod2 provides a protective effect against low levels of ETOH exposure in the developing eye.

ETHANOL HAD A MINIMAL EFFECT ON THE EXPRESSION OF PERIOCCULAR AND OCULAR GENES ASSOCIATED WITH CONGENITAL EYE DISEASES

Malformations of the cornea, iris, and angle structures are associated with mutations in *PITX2* and *FOXC1* (Ozeki et al., 1999; Strungaru et al., 2007; Tumer and Bach-Holm, 2009). Thus, we next investigated the effect of ETOH exposure on the expression of these genes in the periocular mesenchyme and developing eye. Although *pitx2* has

FIGURE 6. Ethanol increased oxidative stress in the facial mesenchyme, but not in the anterior segment. *Tg(sox10:mRFP)* embryos showed that 1% or 3% ETOH treatment starting at 24 hpf increased ROS in *sox10*-positive cells in the facial mesenchyme (arrows, **B,C**) within 2 hr of treatment compared with untreated controls (**A**). In situ hybridization of 36 hpf embryos demonstrated that *sod1* (**D,D'**) and *sod3* (**F,F'**) were expressed in the hyaloid vasculature (arrowheads, **D,F**) and retina in the eye, the periocular mesenchyme, and the facial mesenchyme (open arrow, **D**). *Sod2* was also expressed in the periocular mesenchyme and hyaloid vasculature (arrowhead, **E**). In addition, *sod2* was expressed in the anterior segment of the eye (**E'**) in lens epithelial cells and neural crest cells between the optic cup and surface ectoderm (arrow, **E'**). Semi-quantitative RT-PCR (**G**) of RNA derived from whole 48 hpf embryos showed that 1% ETOH starting at 24 hpf decreased the expression of *sod1* and *sod3*, but increased the expression of *sod2*. Treatment with 3% ETOH from 24 to 48 hpf decreased the expression of *sod1*, *sod2*, and *sod3*. Immunohistochemistry confirmed the expression of *Sod2* protein in the anterior segment (**H**). *Sod2* protein expression was increased by 1% ETOH (**H'**), but decreased by 3% ETOH (**H''**). Knockdown of *Sod2* by MO injection showed decreased protein expression in untreated (**I**), 1% ETOH-treated (**I'**), and 3% ETOH-treated (**I''**) embryos.



multiple isoforms in zebrafish, we previously demonstrated that *pitx2a* is the predominant form responsible for eye development (Bohnsack et al., 2012). There are two isoforms of *foxc1* in zebrafish, *foxc1a* and *foxc1b* (Skarie and Link, 2009). Semi-quantitative RT-PCR showed that 1% or 3% ETOH did not affect the overall expression

of *pitx2a* or *foxc1a* in RNA isolated from whole 48 hpf embryos (Fig. 8A). In situ hybridization, which was used to assess expression pattern in the craniofacial region, showed that 1% or 3% ETOH starting at 24 hpf did not significantly alter *pitx2a* expression in the pituitary (yellow arrows, Fig. 8B, B', and B'') or in the ocular fissure (open arrows, Fig. 8B, B', and B''). In addition, ETOH did not significantly affect the expression pattern of *foxc1a* in the periocular mesenchyme (yellow arrows, Fig. 8C, C', and C'') and within the ocular fissure (open arrows, Fig. 8C, C', and C''). However, treatment with 3% ETOH decreased the overall expression of *foxc1b* in 48 hpf embryos (Fig. 8A), including in the periocular mesenchyme (open arrows, Fig. 8D, D', and D'') and facial mesenchyme (closed arrows, Fig. 7D, D', and D''). These findings show that ETOH affected *foxc1b*, but not *foxc1a* or *pitx2a* in the periocular mesenchyme and developing eye.

Discussion

FAS disorders reflect the disruption of developmental events as a result of prenatal alcohol exposure. The major findings and diagnostic criteria include prenatal and postnatal growth delay, craniofacial anomalies, and central nervous system manifestations (Lemoine et al., 2003; Sokol, 2003; Hoyme et al., 2005; Riley et al., 2011). The eyes and visual system, as an extension of the central nervous system, are often affected (Chan et al., 1991; Stromland and Pinazo-Duran, 2002; Ribeiro et al., 2007; Gummel and Ygge, 2013; Brennan and Giles, 2014; Stromland et al., 2015). The most common intraocular finding is optic nerve hypoplasia, which affects up to 50% of children with FAS and can result in significant visual impairment (Stromland and Pinazo-Duran, 2002; Ribeiro et al., 2007; Abdelrahman and Conn, 2009; Gummel and Ygge, 2013; Brennan and Giles, 2014; Stromland et al., 2015). Microphthalmia (small disorganized globe) is also listed as part of the diagnostic criteria for FAS (Rossett, 1980); however, the prevalence of this condition is more rare (0–5%) in children with FAS (Stromland and Pinazo-Duran,

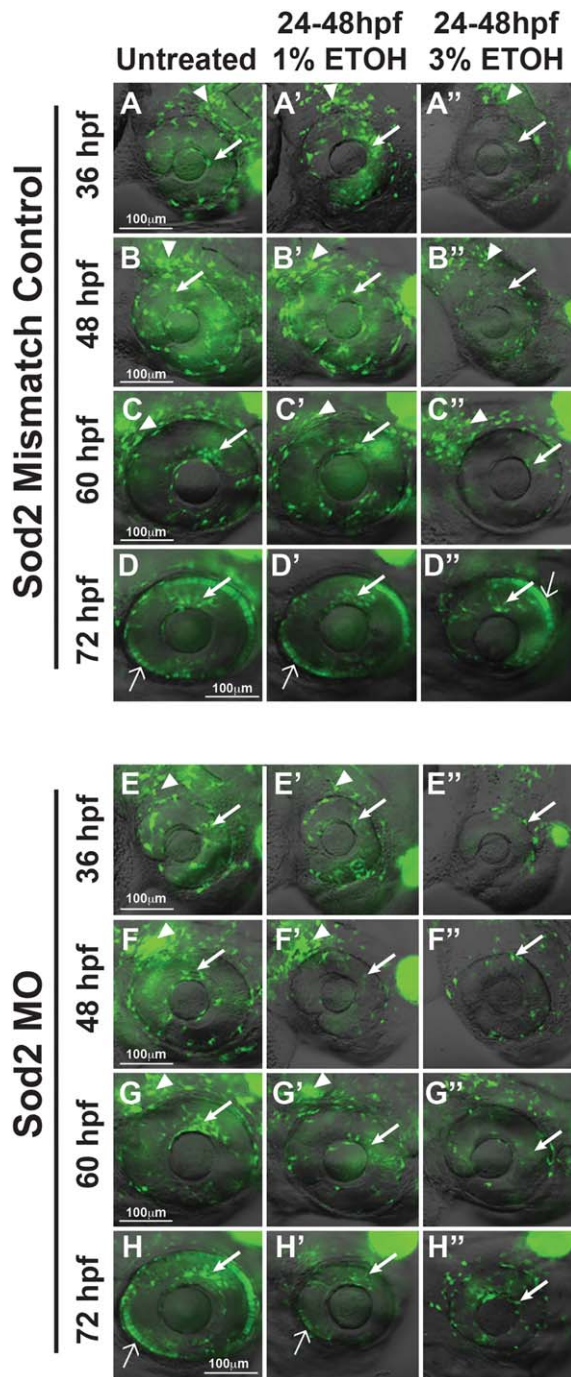


FIGURE 7..

FIGURE 7. *Sod2* decreases effects of ETOH on ocular neural crest and anterior segment development. Live imaging of *Tg(foxd3:GFP)* embryos showed that *foxd3*-positive cell migration into the anterior segment between 36 and 72 hpf (closed arrows, E–H) and *foxd3* expression in photoreceptors (open arrows, H) were not affected by *Sod2* MO knockdown compared with mismatch control-injected (A–D) embryos. Knockdown of *Sod2* in combination with 1% ETOH treatment from 24 to 48 hpf decreased *foxd3*-positive neural crest cell migration into the anterior segment (closed arrows, E'–H'), but did not affect the cells in the periocular mesenchyme (arrowheads, E'–G'). This was in contrast to mismatch control-injected (A'–D') embryos in which 1% ETOH did not affect *foxd3*-positive cells in the periocular mesenchyme (arrowheads, A'–C') or in the anterior segment migration (closed arrows, A'–D'). Treatment with 3% ETOH between 24 and 48 hpf decreased *foxd3*-positive cells in the periocular mesenchyme and in the developing eye in *Sod2* knockdown (E''–H'') and mismatch control-injected (A''–D'') embryos.

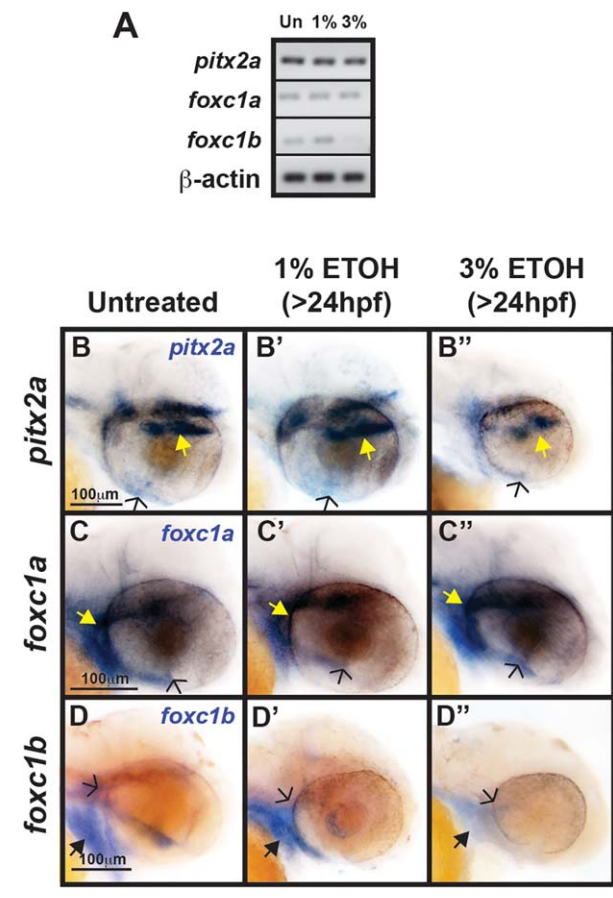


FIGURE 8. Ethanol had a minimal effect on the expression of periocular and ocular genes associated with congenital eye diseases. Semi-quantitative RT-PCR showed that 1% or 3% ETOH treatment from 24 to 48 hpf had minimal effect on expression of *pitx2a*, and *foxc1a* in RNA isolated from whole 48 hpf embryos (A). *Foxc1b* expression was decreased after treatment with 3% ETOH, but not 1% ETOH. Whole-mount in situ hybridization in untreated (B), 1% ETOH treated (B'), and 3% ETOH treated (B'') 48 hpf embryos demonstrated that *pitx2a* was expressed in the pituitary (yellow arrows, B–B''), periocular mesenchyme, and the ocular fissure (black arrows, B–B''). *Foxc1a* was expressed in the facial mesenchyme, periocular mesenchyme (yellow arrows, C–C''), and in the ocular fissure (black arrows, C–C'') of untreated (C), 1% ETOH treated (C'), and 3% ETOH treated (C'') 48 hpf embryos. Similar to *foxc1a*, *foxc1b* was expressed in the facial mesenchyme (solid arrows, D–D'') and periocular mesenchyme (open arrows, D–D''), but not in the ocular fissure of untreated (D) and 1% ETOH treated (D') 48 hpf embryos. Treatment with 3% ETOH decreased *foxc1b* expression (D'') in the facial mesenchyme and periocular mesenchyme.

2002; Ribeiro et al., 2007; Abdelrahman and Conn, 2009; Gummel and Ygge, 2013; Brennan and Giles, 2014; Stromland et al., 2015).

Both optic nerve hypoplasia and microphthalmia reflect disruptions in neuroepithelial-derived optic vesicle formation. Although the neural crest, which gives rise to the cornea, iris, sclera, and angle structures, can be

disrupted in the context of microphthalmia, only 9 cases of isolated anterior segment anomalies in the setting of FAS have been reported (Miller et al., 1984; Edward et al., 1993). In contrast, genetic causes of congenital anomalies often affect both craniofacial structures and anterior development (Ozeki et al., 1999; Aliferis et al., 2010; Dressler et al., 2010). Hence, although craniofacial abnormalities are commonly observed in FAS, the development of the anterior segment of the eye is rarely affected, indicating that ocular neural crest cells are less sensitive to the effects of ETOH than their craniofacial counterparts.

Cellular and molecular differences between the cranial neural crest cells that give rise to craniofacial structures versus those that generate anterior segment structures have not been well defined. Although the molecular characteristics and migratory pathways of the neural crest cells that give rise to the frontonasal process, Meckel's cartilage, ceratohyal cartilage, and pharyngeal arches have been well studied, less is known about the cells destined for the anterior segment of the eye. Both of these cell populations originate from the edge of the neural tube and migrate into the craniofacial region (Trainor, 2005; Dougherty et al., 2012). Our previous studies have shown that cells destined for the anterior segment migrate dorsal and ventral to the eye and populate the periocular mesenchyme (Bohnsack and Kahana, 2013; Chawla et al., 2016). However, specific markers for the cells that enter into the eye have not been previously identified.

In the present study, we observed that *sox10* expression was decreased in the periocular mesenchyme, and few *sox10*-positive cells entered the eye between the surface ectoderm and optic cup. Furthermore, *foxd3* marked a large population of cells entering the anterior segment. Although the majority of these cells migrated into the dorsal–posterior quadrant between the surface ectoderm and optic cup, *foxd3*-positive cells also migrated through the ocular fissure, entering into the anterior segment. Studies in mice, chickens, and humans have not demonstrated this alternative pathway; however, these studies did not use time-lapse live imaging of this migratory cell population. In zebrafish, similar to mice, we did not observe distinct waves of neural crest cells as previously described in humans and chickens (O'Rahilly, 1966, 1975; Hay and Revel, 1969; Pei and Rhodin, 1970). Classic anatomy studies have described three waves of neural crest cells in humans and two waves in chickens. In humans, the first wave contributes to the cornea, the second wave gives rise to the iris, and the third wave forms the angle structures.

While fate mapping has confirmed that these anterior segment structures are derived from the neural crest in chickens and mice, similar studies have not been conducted in zebrafish (Johnston et al., 1979; Noden, 1983; Gage et al., 2005). In the present study, we observed *foxd3*-positive cells in the iris stroma, corneal stroma, and aqueous outflow system in the larval eye, but *foxd3* was

no longer expressed in the adult anterior segment. Additional studies are required to determine the ultimate fate of these cells in the adult eye. Thus, *foxd3* is a marker that demarcates the ocular population of cranial neural crest cells. These studies were necessary for determining differences in ETOH sensitivity between the craniofacial and ocular neural crest populations.

The majority of animal studies focusing on ETOH and ocular development highlight the teratogenic effects on the neuroepithelial-derived optic nerve and retina. These previous studies have recapitulated optic nerve hypoplasia and microphthalmia in different animal models, but have not determined the effect of ETOH on the neural crest cells that contribute to the anterior segment (Cook et al., 1987; Phillips et al., 1991; Pinazo-Duran et al., 1993; Stromland and Pinazo-Duran, 2002). In the present study, we observed that the survival and migration of *foxd3*-positive neural crest cells in the eye were less sensitive to ETOH compared with their *sox10*-positive counterparts destined for craniofacial structures. This difference may in part reflect the increased resistance of periocular and ocular neural crest cells to ROS generation in response to ETOH exposure. Numerous studies have linked the cellular effects of alcohol to increased oxidative stress in both adult and embryonic tissues (Videla et al., 1983; Koch et al., 1991, 2004; Henderson et al., 1995; Heaton et al., 2002; Chu et al., 2007).

The cranial neural crest and developing brain have relatively low levels of antioxidant enzymes compared with the liver or kidneys, making these tissues more susceptible to free radical damage (Davis et al., 1990; Floyd and Carney, 1992; Chen et al., 2000). Indeed, supplementation with antioxidants has been shown to decrease the craniofacial and neurological phenotypes in animal models of FAS (Heaton et al., 2000; Wentzel and Eriksson, 2006; Joya et al., 2015). Ethanol predominantly increases oxidative stress within mitochondria, and as a result, there is a compensatory increase in the expression of the mitochondrial form of superoxide dismutase (*sod2*) in adult tissues (Koch et al., 1994, 2000). Similarly, rat cranial neural crest cells exposed to ETOH show an increase in *Sod2*, but not the soluble (*Sod1*) or extracellular (*Sod3*) forms (Chen and Sulik, 1996; Wentzel and Eriksson, 2006). The results of the present study further revealed that low levels of ETOH, which did not disrupt neural crest migration into the eye, increased the expression of the antioxidant enzyme, *sod2*. Interestingly, this enzyme was highly expressed in the developing anterior segment and knock-down of *Sod2* resulted in increased sensitivity of the ocular neural crest to these low levels of ETOH. In contrast, ETOH decreased the expression of *sod1* and *sod3*, which were expressed in the retina and facial mesenchyme. This suggests a model in which *Sod2* has a protective effect against oxidative stress in the developing anterior segment and this may account for the decreased sensitivity of the

ocular neural crest to ETOH exposure compared with craniofacial neural crest.

The migration, proliferation, and differentiation of neural crest cells that enter into the eye are also regulated through interactions with the optic cup. Retinoic acid is a key regulator that mediates signaling between the developing retina and periocular neural crest. In mice, chickens and zebrafish, retinoic acid is produced in the developing dorsal and ventral retina (Suzuki et al., 2000; Molotkov et al., 2006; Bohnsack et al., 2012). The retinoic acid receptors α , β , and γ are expressed in the periocular mesenchyme, and retinoic acid signaling regulates neural crest cell survival and migration by means of the expression of *Pitx2* and *Foxc1* (Dupe et al., 1999; Matt et al., 2005, 2008; Kumar and Duester, 2010; Bohnsack et al., 2012). Furthermore, tight control of retinoic acid levels is required for proper formation of the iris stroma and cornea in the anterior segment (Bohnsack et al., 2012). Retinoic acid is hypothesized to be a putative target of ethanol through the competitive inhibition of the retinoic acid synthesis enzyme, retinol dehydrogenase (Deltour et al., 1996).

In zebrafish, retinoic acid together with sonic hedgehog can rescue certain phenotypes associated with ethanol exposure, including brain abnormalities, microphthalmia, and retinal differentiation (Muralidharan et al., 2015; Zhang et al., 2016). However, these FAS phenotypes result from neuroepithelial cell anomalies and not neural crest defects. Less is known about the effects of ethanol on retinoic acid in the neural crest, particularly neural crest cell populations in the periocular mesenchyme and developing eye. However, in the present study expression of *pitx2a* and *foxc1a*, which are known targets of retinoic acid, was minimally affected by ETOH exposure suggesting that ETOH may not regulate retinoic acid signaling in the periocular mesenchyme. Prior studies have shown that *pitx2* and *foxc1* are critical for neural crest migration and anterior segment formation (Gage et al., 1999; Kume et al., 2000; Evans and Gage, 2005; Berry et al., 2008; Skarie and Link, 2009; Bohnsack et al., 2012; Chawla et al., 2016). Clinically, gain- or loss-of-function mutations of either of these genes are most commonly associated with Axenfeld-Rieger syndrome, an autosomal dominant congenital disease characterized by anterior segment dysgenesis and craniofacial abnormalities (Strungaru et al., 2007; Tumer and Bach-Holm, 2009; Leis et al., 2012). Taken together, these studies further demonstrated that the neural crest cells around and within the developing eye are more robust to the effects of ETOH and maintain the molecular signals required for anterior segment formation.

The present study assessed the cellular and molecular effects of ETOH on the neural crest cells that form the anterior segment of the eye. Consistent with the rarity of anterior segment abnormalities associated with FAS, the neural crest cell populations in the periocular

mesenchyme and within the developing eye were less sensitive to ETOH exposure compared with the neural crest that gives rise to the jaw and pharyngeal arches. These studies provide further insight into the pathogenesis of congenital anomalies and the effects of prenatal alcohol exposure on craniofacial and ocular development.

Acknowledgments

The authors thank the Kellogg Eye Center Morphology and Imaging Module for technical assistance.

References

- Abdelrahman A, Conn R. 2009. Eye abnormalities in fetal alcohol syndrome. *Ulster Med J* 78:164–165.
- Aliferis K, Marsal C, Pelletier V, et al. 2010. A novel nonsense B3GALT1 mutation confirms Peters plus syndrome in a patient with multiple malformations and Peters anomaly. *Ophthalmic Genet* 31:205–208.
- Barthel LK, Raymond PA. 2000. In situ hybridization studies of retinal neurons. *Methods Enzymol* 316:579–590.
- Berry FB, Skarie JM, Mirzayans F, et al. 2008. FOXC1 is required for cell viability and resistance to oxidative stress in the eye through the transcriptional regulation of FOXO1A. *Hum Mol Genet* 17:490–505.
- Bohnsack BL, Gallina D, Kahana A. 2011a. Phenothiourea sensitizes zebrafish cranial neural crest and extraocular muscle development to changes in retinoic acid and insulin-like growth factor signaling. *PLoS One* 6:e22991.
- Bohnsack BL, Gallina D, Thompson H, et al. 2011b. Development of extraocular muscles require early signals from periocular neural crest and the developing eye. *Arch Ophthalmol* 129:1030–1041.
- Bohnsack BL, Kahana A. 2013. Thyroid hormone and retinoic acid interact to regulate zebrafish craniofacial neural crest development. *Dev Biol* 373:300–309.
- Bohnsack BL, Kasprick D, Kish PE, et al. 2012. A zebrafish model of Axenfeld-Rieger Syndrome reveals that *pitx2* regulation by retinoic acid is essential for ocular and craniofacial development. *Invest Ophthalmol Vis Sci* 53:7–22.
- Brennan D, Giles S. 2014. Ocular involvement in fetal alcohol spectrum disorder: a review. *Curr Pharm Des* 20:5377–5387.
- Chan T, Howell R, O'Keefe M, Lanigan B. 1991. Ocular manifestations in fetal alcohol syndrome. *Br J Ophthalmol* 75:524–526.
- Chawla B, Schley E, Williams AL, Bohnsack BL. 2016. Retinoic acid and *pitx2* regulate early neural crest survival and migration in craniofacial and ocular development. *Birth Defects Res B Dev Reprod Toxicol* 107:126–135.
- Chen SY, Periasamy A, Yang B, et al. 2000. Differential sensitivity of mouse neural crest cells to ethanol-induced toxicity. *Alcohol* 20:75–81.
- Chen SY, Sulik KK. 1996. Free radical and ethanol-induced cytotoxicity in neural crest cells. *Alcohol Clin Exp Res* 20:1071–1076.
- Chu J, Tong M, de la Monte SM. 2007. Chronic ethanol exposure causes mitochondrial dysfunction and oxidative stress in immature central nervous system neurons. *Acta Neuropathol* 113:659–673.
- Clarren SK, Alvord ECJ, Sumi SM, et al. 1978. Brain malformations related to prenatal exposure to ethanol. *J Pediatr* 92:64–67.
- Cook C, Nowotny AZ, Sulik KK. 1987. Fetal alcohol syndrome. Eye malformations in a mouse model. *Arch Ophthalmol* 105:1576–1580.
- Creuzet S, Vincent C, Couly G. 2005. Neural crest derivatives in ocular and periocular structures. *Int J Dev Biol* 49:161–171.
- Curran K, Raible DW, Lister JA. 2009. Foxd3 controls melanophore specification in the zebrafish neural crest by regulation of Mitf. *Dev Biol* 332:408–417.
- Davis WL, Crawford LA, Cooper OJ, et al. 1990. Ethanol induces the generation of reactive free radicals by neural crest cells in vitro. *J Craniofac Genet Dev Biol* 10:288–293.
- Deltour L, Ang HL, Duester G. 1996. Ethanol inhibition of retinoic acid synthesis as a potential mechanism for fetal alcohol syndrome. *FASEB J* 10:1050–1057.
- Dougherty M, Kamel G, Shubinets V, et al. 2012. Embryonic fate map of first pharyngeal arch structures in the *sox10:kaede* zebrafish transgenic model. *J Craniofac Surg* 23:1333–1337.
- Dressler S, Meyer-Marcotty P, Weisschuh N, et al. 2010. Dental and craniofacial anomalies associated with Axenfeld-Rieger syndrome with PITX2 mutation. *Case Report Med* 2010:621984.
- Dunty WCJ, Zucker RM, Sulik KK. 2002. Hindbrain and cranial nerve dysmorphogenesis result from acute maternal ethanol administration. *Dev Neurosci* 24:328–342.
- Dupe V, Ghyselinck NB, Wendling O, et al. 1999. Key roles of retinoic acid receptors alpha and beta in the patterning of the caudal hindbrain, pharyngeal arches and otocyst in the mouse. *Development* 126:5051–5059.
- Dutton K, Dutton JR, Pauliny A, Kelsh RN. 2001a. A morpholino phenocopy of the colourless mutant. *Genesis* 30:188–189.
- Dutton KA, Pauliny A, Lopes SS, et al. 2001b. Zebrafish colourless encodes *sox10* and specifies non-ectomesenchymal neural crest fates. *Development* 128:4113–4125.
- Edward DP, Li J, Sawaguchi S, et al. 1993. Diffuse corneal clouding in siblings with fetal alcohol syndrome. *Am J Ophthalmol* 15:484–493.

- Evans AL, Gage PJ. 2005. Expression of the homeobox gene *Pitx2* in neural crest is required for optic stalk and ocular anterior segment development. *Hum Mol Genet* 14:3347–3359.
- Flentke GR, Garic A, Amberger E, et al. 2011. Calcium-mediated repression of beta-catenin and its transcriptional signaling mediates neural crest cell death in an avian model of fetal alcohol syndrome. *Birth Defects Res A Clin Mol Teratol* 91:591–602.
- Floyd RA, Carney JM. 1992. Free radical damage to protein and DNA: mechanisms involved and relevant observations on brain undergoing oxidative stress. *Ann Neurol* 32(Suppl):S22–S27.
- Foroud T, Wetherill L, Vinci-Booher S, et al. 2012. Relation over time between facial measurements and cognitive outcomes in fetal alcohol-exposed children. *Alcohol Clin Exp Res* 36:1634–1646.
- Gage PJ, Rhoades W, Prucka SK, Hjalt T. 2005. Fate maps of neural crest and mesoderm in the mammalian eye. *Invest Ophthalmol Vis Sci* 46:4200–4208.
- Gage PJ, Suh H, Camper SA. 1999. Dosage requirement of *Pitx2* for development of multiple organs. *Development* 126:4643–4651.
- Garic A, Flentke GR, Amberger E, et al. 2011. CaMKII activation is a novel effector of alcohol's neurotoxicity in neural crest stem/progenitor cells. *J Neurochem* 118:646–657.
- Garic-Stankovic A, Hernandez M, Flentke GR, Smith SM. 2005. Ethanol triggers neural crest apoptosis through the selective activation of a pertussis toxin-sensitive G protein and a phospholipase C-beta-dependent Ca²⁺ transient. *Alcohol Clin Exp Res* 29:1237–1246.
- Gummel K, Ygge J. 2013. Ophthalmologic findings in Russian children with fetal alcohol syndrome. *Eur J Ophthalmol* 23:823–830.
- Hay ED, Revel JP. 1969. Fine structure of the developing avian cornea. *Monogr Dev Biol* 1:1–144.
- Heaton MB, Mitchell JJ, Paiva M. 2000. Amelioration of ethanol-induced neurotoxicity in the neonatal rat central nervous system by antioxidant therapy. *Alcohol Clin Exp Res* 24:512–518.
- Heaton MB, Paiva M, Mayer J, Miller R. 2002. Ethanol-mediated generation of reactive oxygen species in developing rat cerebellum. *Neurosci Lett* 334:83–86.
- Henderson GI, Devi GB, Perez A, Schenker S. 1995. In utero ethanol exposure elicits oxidative stress in the rat fetus. *Alcohol Clin Exp Res* 19:714–720.
- Honoré SM, Aybar MJ, Mayor R. 2003. *Sox10* is required for the early development of the prospective neural crest in *Xenopus* embryos. *Dev Biol* 260:79–96.
- Hoyme HE, May PA, Kalberg WO, et al. 2005. A practical clinical approach to diagnosis of fetal alcohol syndrome disorders: clarification of the 1996 institute of medicine criteria. *Pediatrics* 115:39–47.
- Johnston MC. 1966. A radioautographic study of the migration and fate of cranial neural crest cells in the chick embryo. *Anat Rec* 156:143–155.
- Johnston MC, Noden DM, Hazelton RD, et al. 1979. Origins of avian ocular and periocular tissues. *Exp Eye Res* 29:27–43.
- Jones KL, Smith DW, Ulleland CN, Streissguth P. 1973. Pattern of malformation in offspring of chronic alcoholic mothers. *Lancet* 1:1267–1271.
- Joya X, Garcia-Algar O, Salat-Batlle J, et al. 2015. Advances in the development of novel antioxidant therapies as an approach for fetal alcohol syndrome prevention. *Birth Defects Res Part A Clin Mol Teratol* 103:163–177.
- Joya X, Garcia-Algar O, Vall O, Pujades C. 2014. Transient exposure to ethanol during zebrafish embryogenesis results in defects in neuronal differentiation: an alternative model system to study FASD. *PLoS One* 9:e112851.
- Kajimura S, Aida K, Duan C. 2005. Insulin-like growth factor-binding protein-1 (IGFBP-1) mediates hypoxia-induced embryonic growth and developmental retardation. *Proc Natl Acad Sci U S A* 102:1240–1245.
- Kiecker C. 2016. The chick embryo as a model for the effects of prenatal exposure to alcohol on craniofacial development. *Dev Biol* 415:314–325.
- Kimmel CB, Ballard WW, Kimmel SR, et al. 1995. Stages of embryonic development of the zebrafish. *Dev Dyn* 203:253–310.
- Klingenberg CP, Wetherill L, Rogers J, et al. 2010. Prenatal alcohol exposure alters the patterns of facial asymmetry. *Alcohol* 44:649–657.
- Koch OR, De Leo ME, Borrello S, et al. 1994. Ethanol treatment up-regulates the expression of mitochondrial manganese superoxide dismutase activity in rat liver. *Biochem Biophys Res Commun* 201:1356–1365.
- Koch OR, Farre S, De Leo ME, et al. 2000. Regulation of manganese superoxide dismutase (Mn-SOD) in chronic-experimental alcoholism: effects of vitamin E-supplemented and deficient diets. *Alcohol* 35:159–163.
- Koch OR, Galeotti T, Bartoli GM, Boveris A. 1991. Alcohol-induced oxidative stress in rat liver. *Xenobiotica* 21:1077–1084.
- Koch OR, Pani G, Borrello S, et al. 2004. Oxidative stress and antioxidant defenses in ethanol-induced cell injury. *Mol Aspects Med* 25:191–198.
- Kucenas S, Takada N, Park HC, et al. 2008. CNS-derived glia ensheath peripheral nerves and mediate motor root development. *Nat Neurosci* 11:143–151.
- Kumar S, Duester G. 2010. Retinoic acid signaling in periocular mesenchyme represses Wnt signaling via induction of *Pitx2* and *Dkk2*. *Dev Biol* 340:67–74.

- Kume T, Deng K, Hogan BL. 2000. Murine forkhead/winged helix genes *Foxc1* (Mf1) and *Foxc2* (Mfh) are required for the early organogenesis of the kidney and urinary tract. *Development* 127:1387–1395.
- Kwak J, Park OK, Jung YK, et al. 2013. Live imaging profiling of neural crest lineages in zebrafish transgenic lines. *Mol Cells* 35:255–260.
- Leis LM, Tyler RC, Volkmann Kloss BA, et al. 2012. PITX2 and FOXC1 spectrum of mutations in ocular syndromes. *Eur J Hum Genet* 20:1224–1233.
- Lemoine P, Harousseau H, Borteyru JP, Menuet JC. 2003. Children of alcoholic parents - observed anomalies: discussion of 127 cases. *Ther Drug Monit* 25:132–136.
- Lesnik Oberstein SA, Kriek M, White SJ, et al. 2006. Peters Plus syndrome is caused by mutations in B3GALTL, a putative glycosyltransferase. *Am J Hum Genet* 79:562–566.
- Lovely CB, Fernandes Y, Eberhart JK. 2016. Fishing for fetal alcohol spectrum disorders: zebrafish as a model for ethanol teratogenesis. *Zebrafish* 13:391–398.
- Maier SE, Chen WJ, Miller JA, West JR. 1997. Fetal alcohol exposure and temporal vulnerability regional differences in alcohol-induced microencephaly as a function of the timing of binge-like alcohol exposure during rat brain development. *Alcohol Clin Exp Res* 21:1418–1428.
- Maier SE, Miller JA, Blackwell JM, West JR. 1999. Fetal alcohol exposure and temporal vulnerability: regional differences in cell loss as a function of the timing of binge-like alcohol exposure during brain development. *Alcohol Clin Exp Res* 23:726–734.
- Matt N, Dupe V, Garnier J-M, et al. 2005. Retinoic acid-dependent eye morphogenesis is orchestrated by neural crest cells. *Development* 132:4789–4800.
- Matt N, Ghyselinck NB, Pellerin I, Dupe V. 2008. Impairing retinoic acid signalling in the neural crest cells is sufficient to alter entire eye morphogenesis. *Dev Biol* 320:140–148.
- Mattson SN, Riley EP. 1996. In: Abel EL, editor. *Brain anomalies in fetal alcohol syndrome*. Boca Raton, FL: CRC Press. pp. 50–68.
- Miller MT, Epstein RJ, Sugar J, et al. 1984. Anterior segment anomalies associated with the fetal alcohol syndrome. *J Pediatr Ophthalmol Strabismus* 21:8–18.
- Molotkov A, Molotkova N, Duyster G. 2006. Retinoic acid guides eye morphogenetic movements via paracrine signaling but is unnecessary for retinal dorsoventral patterning. *Development* 133:1901–1910.
- Montero-Balaguer M, Lang MR, Sachdev SW, et al. 2006. The mother superior mutation ablates *foxd3* activity in neural crest progenitor cells and depletes neural crest derivatives in zebrafish. *Dev Dyn* 235:3199–3212.
- Mugoni V, Camporeale A, Santoro MM. 2014. Analysis of oxidative stress in zebrafish embryos. *J Vis Exp* 89:e51328.
- Muralidharan P, Sarmah S, Marrs JA. 2015. Zebrafish retinal defects induced by ethanol exposure are rescued by retinoic acid and folic acid supplement. *Alcohol* 49:149–163.
- Noden DM. 1983. The role of the neural crest in patterning of avian cranial skeletal, connective, and muscle tissues. *Dev Biol* 96:144–165.
- O’Rahilly R. 1966. The early development of the eye in staged human embryos. *Contrib Embryol Carneg Inst* 38:1–42.
- O’Rahilly R. 1975. The prenatal development of the human eye. *Exp Eye Res* 21:93–112.
- Ozeki H, Shirai S, Ikeda K, Ogura Y. 1999. Anomalies associated with Axenfeld-Rieger syndrome. *Graefes Arch Clin Exp Ophthalmol* 237:730–734.
- Parnell SE, O’Leary-Moore SK, Godin EA, et al. 2009. Magnetic resonance microscopy defines ethanol-induced brain abnormalities in prenatal mice: effects of acute insult on gestational day 8. *Alcohol Clin Exp Res* 33:1001–1011.
- Pei YF, Rhodin JA. 1970. The prenatal development of the mouse eye. *Anat Rec* 168:105–125.
- Peterman EM, Sullivan C, Goody ME, et al. 2015. Neutralization of mitochondrial superoxide by superoxide dismutase 2 promotes bacterial clearance and regulates phagocyte numbers in zebrafish. *Infect Immun* 83:430–440.
- Phillips DE, Krueger SK, Rydquist JE. 1991. Short- and long-term effects of combined pre- and postnatal ethanol exposure (three trimester equivalency) on the development of myelin and axons in the optic nerve. *Int J Dev Neurosci* 9:631–647.
- Pinazo-Duran MD, Renau-Piqueras J, Guerri C. 1993. Developmental changes in the optic nerve related to ethanol consumption in pregnant rats: analysis of the ethanol-exposed optic nerve. *Teratology* 48:305–322.
- Ribeiro IM, Vale PJ, Tenedorio PA, et al. 2007. Ocular manifestations in fetal alcohol syndrome. *Eur J Ophthalmol* 17:104–109.
- Riley EP, Infante MA, Warren KR. 2011. Fetal alcohol spectrum disorders: an overview. *Neuropsychol Rev* 21:73–80.
- Rossett HL. 1980. A clinical perspective of the fetal alcohol syndrome. *Alcohol Clin Exp Res* 4:119–122.
- Sampson PD, Streissguth AP, Bookstein FL, et al. 1997. Incidence of fetal alcohol syndrome and prevalence of alcohol-related neurodevelopmental disorder. *Teratology* 56:317–326.
- Schoner K, Kohlhase J, Müller AM, et al. 2013. Hydrocephalus, agenesis of the corpus callosum, and cleft lip/palate represent frequent associations in fetuses with Peters plus syndrome and B3GALTL mutations. Fetal PPS phenotypes, expanded by Dandy Walker cyst and encephalocele. *Prenat Diagn* 33:75–80.
- Skarie JM, Link BA. 2009. FoxC1 is essential for vascular basement membrane integrity and hyaloid vessel morphogenesis. *Invest Ophthalmol Vis Sci* 50:5026–5034.

- Smith SM, Garic A, Flentke GR, Berres ME. 2014. Neural crest development in fetal alcohol syndrome. *Birth Defects Res Part C Embryol Today* 102:210–220.
- Sokol RJ. 2003. Fetal alcohol syndrome disorder. *JAMA* 290:2996–2999.
- Stewart RA, Arduini BL, Berghmans S, et al. 2006. Zebrafish *foxd3* is selectively required for neural crest specification, migration and survival. *Dev Biol* 292:174–188.
- Stromland K. 1987. Ocular involvement in the fetal alcohol syndrome. *Surv Ophthalmol* 31:277–284.
- Stromland K, Pinazo-Duran MD. 2002. Ophthalmic involvement in the fetal alcohol syndrome: clinical and animal model studies. *Alcohol Alcohol* 37:2–8.
- Stromland K, Ventura LO, Mirzaei L, et al. 2015. Fetal alcohol spectrum disorders among children in Brazilian orphanage. *Birth Defects Res Part A Clin Mol Teratol* 103:178–185.
- Strungaru MH, Dinu I, Walter MA. 2007. Genotype-phenotype correlations in Axenfeld-Rieger malformation and glaucoma patients with *FOXC1* and *PITX2* mutations. *Invest Ophthalmol Vis Sci* 48:228–237.
- Sulik KK, Johnson MC, Webb MA. 1981. Fetal alcohol syndrome: embryogenesis in a mouse model. *Science* 214:936–938.
- Sulik KK, Lauder JM, Dehart DB. 1984. Brain malformations in prenatal mice following acute maternal ethanol administration. *Int J Dev Neurosci* 2:203–214.
- Suzuki R, Shintani T, Sakuta H, et al. 2000. Identification of *RALDH-3* a novel retinaldehyde dehydrogenase, expressed in the ventral region of the retina. *Mech Dev* 98:37–50.
- Tolosa EJ, Fernández-Zapico ME, Battiato NL, Rovasio RA. 2016. Sonic hedgehog is a chemotactic neural crest cell guide that is perturbed by ethanol exposure. *Eur J Cell Biol* 95:136–152.
- Trainor PA. 2005. Specification of neural crest cell formation and migration in mouse embryos. *Sem Cell Dev Biol* 16:683–693.
- Trainor PA, Tam PPL. 1995. Cranial paraxial mesoderm and neural crest cells of the mouse embryo-codistribution in the craniofacial mesenchyme but distinct segregation in branchial arches. *Development* 121:2569–2582.
- Tumer Z, Bach-Holm D. 2009. Axenfeld-Rieger syndrome and spectrum of *Pitx2* and *Foxc1* mutations. *Eur J Hum Genet* 17:1527–1539.
- Videla LA, Fraga CG, Koch OR, Boveris A. 1983. Chemiluminescence of the in situ rat liver after acute ethanol intoxication. Effect of (+)-cyanidanol-3. *Biochem Pharmacol* 32:2822–2825.
- Wentzel P, Eriksson UJ. 2006. Ethanol-induced fetal dysmorphogenesis in the mouse is diminished by high antioxidative capacity of the mother. *Toxicol Sci* 92:416–422.
- Williams AL, Eason J, Chawla B, Bohnsack BL. 2017. *Cyp1b1* regulates ocular fissure closure through a retinoic acid-independent pathway. *Invest Ophthalmol Vis Sci* 58:1084–1097.
- Zhang C, Anderson A, Cole GJ. 2016. Analysis of crosstalk between retinoic acid and sonic hedgehog pathways following ethanol exposure in embryonic zebrafish. *Birth Defects Res Part A* 103:1046–1067.
- Zhang C, Frazier JM, Chen H, et al. 2014. Molecular and morphological changes in zebrafish following transient ethanol exposure during defined developmental stages. *Neurotoxicol Teratol* 44:70–80.